Moist synoptic transport of CO_2 along the mid-latitude storm track

N. C. Parazoo,[1] A. S. Denning,[1] J. A. Berry,[2] A. Wolf,[3] D. A. Randall,[1] S. R. Kawa,[4] O. Pauluis,[5] and S. C. Doney[6]

Received 22 February 2011; revised 30 March 2011; accepted 1 April 2011; published 12 May 2011.

[1] Atmospheric mixing ratios of CO_2 are strongly seasonal in the Arctic due to mid-latitude transport. Here we analyze the seasonal influence of moist synoptic storms by diagnosing CO_2 transport from a global model on moist isentropes (to represent parcel trajectories through stormtracks) and parsing transport into eddy and mean components. During winter when northern plants respire, warm moist air, high in CO_2, is swept poleward into the polar vortex, while cold dry air, low in CO_2, that had been transported into the polar vortex earlier in the year is swept equatorward. Eddies reduce seasonality in mid-latitudes by ~50% of NEE (~100% of fossil fuel) while amplifying seasonality at high latitudes. Transport along stormtracks is correlated with rising, moist, cloudy air, which systematically hides this CO_2 transport from satellites. We recommend that (1) regional inversions carefully account for meridional transport and (2) inversion models represent moist and frontal processes with high fidelity. **Citation:** Parazoo, N. C., A. S. Denning, J. A. Berry, A. Wolf, D. A. Randall, S. R. Kawa, O. Pauluis, and S. C. Doney (2011), Moist synoptic transport of CO_2 along the mid-latitude storm track, *Geophys. Res. Lett.*, *38*, L09804, doi:10.1029/2011GL047238.

1. Introduction

[2] It has long been recognized that seasonal and diurnal covariance between terrestrial ecosystem metabolism and fine-scale vertical transport in the atmosphere is a strong determinant of vertical structure in CO_2 mixing ratio (the "CO_2 rectifier" [e.g., *Denning et al.*, 1995]). Like the CO_2 rectifier, synoptic transport by baroclinic waves along the mid-latitude storm track involves strong vertical motion and is correlated with ecosystem metabolism because large-scale baroclinicity and photosynthesis are both driven seasonally by variations in solar radiation. Baroclinic wave activity is enhanced in winter when respiration and decomposition dominate ecosystem metabolism, and is suppressed in summer when photosynthesis dominates.

[1]Department of Atmospheric Science, Colorado State University, Fort Collins, Colorado, USA.
[2]Department of Global Ecology, Carnegie Institution of Washington, Stanford, California, USA.
[3]Department of Ecology and Evolutionary Biology, Princeton University, Princeton, New Jersey, USA.
[4]NASA Goddard Space Flight Center, Greenbelt, Maryland, USA.
[5]Courant Institute of Mathematical Sciences, New York University, New York, New York, USA.
[6]Woods Hole Oceanographic Institution, Woods Hole, Massachusetts, USA.

Copyright 2011 by the American Geophysical Union.
0094-8276/11/2011GL047238

[3] Unlike the CO_2 rectifier, tracer transport by "slantwise convection" in baroclinic waves involves a strong meridional component and is intimately tied to condensation and precipitation processes. A recent analysis by *Pauluis et al.* [2008] found that mass transport along moist isentropic surfaces on baroclinic waves represents an important component of the atmospheric heat engine that operates between the equator and poles. This is also an important vehicle for tracer transport. Poleward transport by rising warm moist air follows a "warm conveyor belt (WCB)" above warm fronts, and is compensated by equatorward transport by sinking cold dry air following a "dry air intrusion (DI)" behind cold fronts [*Cooper et al.*, 2001; *Stohl*, 2001].

[4] Pollution transport by WCBs has received much attention in the scientific literature. *Carlson* [1981] presented empirical evidence indicating aerosol transport into the Arctic along moist isentropic surfaces. More recently, models and aircraft measurements from intensive field campaigns (e.g., North American Regional Experiment) have helped create conceptual models that explain how WCBs transport gases such as O_3 and CO upward, poleward, and eastward away from continents and across ocean basins [e.g., *Bethan et al.*, 1998; *Cooper et al.*, 2001]. Strong pollution transport by WCBs is not surprising considering WCBs originate near the surface in polluted boundary layers and are responsible for most of a mid-latitude cyclone's meridional energy transport [*Eckhardt et al.*, 2004].

[5] CO_2 transport by baroclinic waves was described in detail by *Fung et al.* [1983] and was included in the study by *Tans et al.* [1990] that established the concept of a terrestrial carbon sink but has not received much attention since (however, see *Miyazaki et al.* [2008] and *Keppel-Aleks et al.* [2011]). Here we refine our understanding of synoptic transport of CO_2 by including the contribution from moist processes embedded within stormtracks. Analysis of global transport simulations on moist isentropes (described in Section 2) provides a means for describing how synchrony of baroclinic disturbances with ecosystem metabolism modulates seasonal variations of CO_2 in northern mid-latitudes. We use "eddy decomposition," discussed in more detail in Section 2, to isolate transport signals associated with baroclinic waves. In Section 3 we discuss the influence of mean and eddy components of the atmospheric circulation on seasonal variations of CO_2, and in Section 4 discuss implications of moist synoptic transport for CO_2 inversions.

2. Methods

[6] Transport of seasonally varying CO_2 is analyzed in the global Parameterized Chemistry and Transport Model

(PCTM) [*Kawa et al.*, 2004], with transport driven by the Goddard EOS Data Assimilation System (GEOS4) from 2005–06 (years for which moisture data is available). Surface fluxes include net ecosystem exchange and fossil fuel emissions, which are described by *Parazoo et al.* [2008], and simulated air-sea exchange as described by *Doney et al.* [2009].

[7] The temporally-zonally averaged, vertically integrated tendency equation for CO_2 is

$$\frac{\partial}{\partial t}\int_{\zeta_{toa}}^{\zeta_{sfc}}\left[\overline{m_\zeta C_\zeta}\right]d\zeta+\frac{1}{a\cos\phi}\frac{\partial}{\partial\phi}\int_{\zeta_{toa}}^{\zeta_{sfc}}\left[\overline{m_\zeta v_\zeta C_\zeta}\right]\cos\phi d\zeta=\left[\overline{(F_C)_{sfc}}\right], \quad (1)$$

where ζ is an arbitrary vertical coordinate, C is CO_2 mixing ratio, $m_\zeta = \frac{1}{g}\frac{\partial p}{\partial \zeta}$ is the pseudo-density, a is the radius of Earth, φ is latitude, v is the meridional wind, g is gravity, p is pressure, and $(F_C)_{sfc}$ is the surface flux of CO_2. $\overline{(\ )}$ refers to time averages and [( )] to zonal averages. Equation (1) reduces to the continuity equation for total mass (air) by setting C to unity and $(F_C)_{sfc}$ to zero; for total mass, net meridional transport averages to zero over a sufficiently long time.

[8] The large-scale mid-latitude circulation is unstable to the extent that strong zonal and temporal asymmetries from the zonally symmetric circulation arise. To assess influences of zonally symmetric, or "mean" circulations, and asymmetric, or "eddy" circulations, on meridional transport of CO_2, eddy decomposition is applied to $\left[\overline{m_\zeta v_\zeta C_\zeta}\right]$ following *Peixoto and Oort* [1992]. Time and spatially varying atmospheric quantities are parsed into mean and eddy components, where $x = \overline{x} + x'$ represents the time mean and its temporal deviation $(\ )'$ and $x = [x] + x^*$ represents the zonal mean and its zonal deviation $(\ )^*$. By separating $m_\zeta v_\zeta$ and C into mean and eddy components, $\left[\overline{m_\zeta v_\zeta C_\zeta}\right]$ is expressed as

$$\left[\overline{m_\zeta v_\zeta C_\zeta}\right]=\left[\overline{m_\zeta v_\zeta}\right]\left[\overline{C_\zeta}\right]+\left[\overline{m_\zeta v_\zeta}^*\overline{C_\zeta}^*\right]+\left[\overline{(m_\zeta v_\zeta)'C_\zeta'}\right]. \quad (2)$$

Eddy decomposition is an extension of Reynolds averaging and applies to the large-scale, geostrophically and hydrostatically balanced flow. The focus of this study is transport by baroclinic waves, which occurs over scales of 3–7 days and ~1000 km. Monthly averaging is applied to capture the net effect of eddies over multiple synoptic cycles. Through these averaging techniques, CO_2 transport is expressed as meridional and vertical statistics.

[9] The first RHS term in equation (2) refers to the mean meridional circulation, and accounts for transport of mean CO_2 by the mean meridional mass flux. The second term refers to stationary eddies and represents transport by stationary waves due to correlated zonal deviations of mass flux and CO_2. These are forced by the geographic anchoring of planetary scale atmospheric waves by zonal inhomogeneities in boundary conditions such as continents, oceans and mountains. The third term accounts for temporal variations from stationary waves, or transient eddies, and represents transport by time varying dynamical processes due to correlated temporal variations of mass flux and CO_2. In mid-latitudes, baroclinic instability is a major driver of transient eddies. Transport by transient and stationary waves together represents the eddy component of the large-scale mid-latitude circulation.

[10] Our choice of vertical coordinate is crucial for describing horizontal and vertical components of motion associated with these processes. Isentropic surfaces, defined as either dry ($\theta = T\left(\frac{p_o}{p}\right)^{\frac{R}{c_p}}$, with θ the potential temperature, T the temperature, p the pressure, p_o = 1000 mb the reference pressure, R the ideal gas constant, and C_p the specific heat) or moist ($\theta_e \sim \theta + \frac{L_v}{c_p}q$, with q the water vapor concentration and L_v the latent heat of vaporization), are popular because they are more indicative of parcel trajectories through stormtracks than Eulerian averages [e.g., *Townsend and Johnson*, 1985]. Horizontal flow along isentropes contains (approximately) the adiabatic component of vertical motion (assuming radiative cooling and sensible heating are relatively unimportant for synoptic motions) that is often excluded from Eulerian reference systems. An advantage of θ_e over θ is that it's approximately conserved (moist static energy neither lost nor gained) in the presence of latent heating. Mass transport on θ_e therefore includes a large contribution from moist air rising within stormtracks [*Pauluis et al.*, 2008], while other forms of averaging misses entirely this contribution (the corresponding transport ends up in the mean term). The vertical component of motion gained from latent heat release in condensing moist air is critical for describing tracer transport by moist ascent within synoptic waves. We therefore set $\zeta = \theta_e$ in equation (2) and compute mean and eddy transport of CO_2 on θ_e.

3. Results

[11] Vertical distributions of mean and eddy transport of CO_2 on θ_e, including vertical sums, are summarized in Figure 1. Poleward and equatorward transport by the mean meridional flow largely cancel one another (Figure 1a) with smaller residual equatorward transport in the column (Figure 1b). During boreal winter, the northern mid-latitudes are a source region for CO_2 through ecosystem respiration and fossil fuel emission such that CO_2 accumulates near the surface. Transport by the mean circulation leads to mean poleward transport of relatively low CO_2 (with respect to the vertical mean) at large θ_e (corresponding approximately to the upper troposphere in an isentropically stable atmosphere) and equatorward transport of relatively high CO_2 at small θ_e (near the surface), consistent with *Miyazaki et al.* [2008]. Column integrated transport by the mean circulation is equatorward (Figure 1b), reflecting the interplay of the strong vertical CO_2 gradient and the single overturning cell exhibited in the mean circulation field on θ_e.

[12] Eddy transport is weaker, by several orders of magnitude, but poleward through most of the troposphere (Figure 1c), opposing mean transport in the vertical integral (Figure 1d). Eddy transport is forced through covariance between perturbations (temporal and zonal) to the mean circulation and to mean CO_2. Positive (negative) perturbations to the mean circulation represent anomalous poleward (equatorward) mass flux, with poleward flow of warm moist air (θ_e > ~280K) representing WCBs and equatorward flow of cold dry air (θ_e < ~280K) representing DIs. Anomalous mass flux along θ_e causes corresponding perturbations to mean CO_2 (with respect to latitude). Because CO_2 decreases northward on θ_e throughout much of the troposphere,

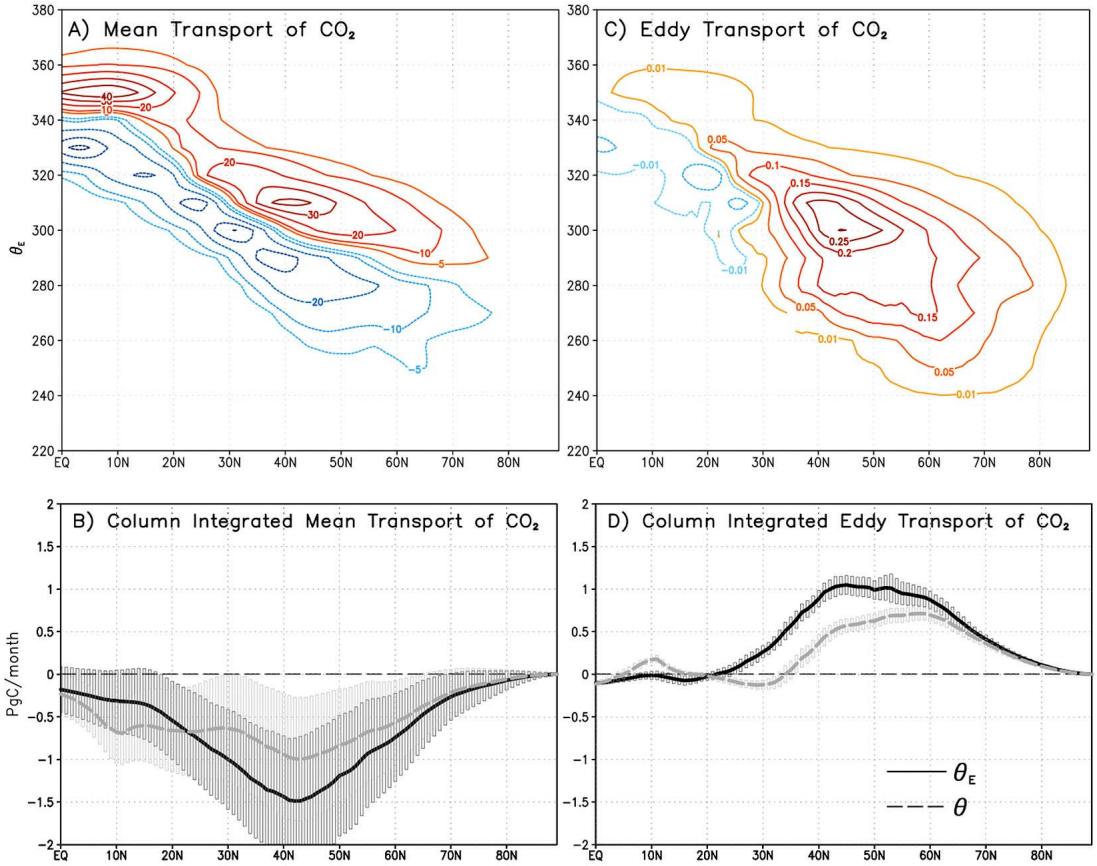

Figure 1. Winter (Dec–Feb) CO_2 transport by the (a, b) mean meridional circulation and (c, d) eddies, distributed vertically along θ_e (Figures 1a and 1c) and combined into total column integrated transport (Figures 1b and 1d) along θ_e(solid black line) and θ (dashed grey line). Shading in Figures 1b and 1d indicates the root mean squared error. Figures 1a and 1c have units of PgC month^{-1} K^{-1} and Figures 1b and 1d have units of PgC month^{-1}. Positive values indicate northward transport.

anomalous poleward mass flux causes positive perturbations of CO_2. Positive covariance of these quantities results in net poleward transport. Net eddy transport is poleward throughout the column (Figure 1c) and in the column integral (Figure 1d) during winter.

[13] Examination of a particular case illustrates the eddy transport mechanism. A composite surface map (Figure 2a) shows an extratropical cyclone that passed over the continental United States (U. S.) on 13 January 2005. A low-pressure system is centered over Lake Michigan, with corresponding warm and stationary fronts (solid red line and red-blue line, respectively) passing into New England and a cold front (solid blue line) over the Great Plains extending to Mexico. In the warm sector of the cyclone (southeast U. S.) there is poleward flow (depicted by wind vectors at surface stations pointing north) of warm moist air (temperatures from 10–20°C, high dewpoints). Following the classic mid-latitude cyclone [*Cooper et al.*, 2001; *Stohl*, 2001], this air follows a WCB, rises above the surface warm front, and spreads into Canada and the Atlantic. In the cold sector is equatorward flow (wind vectors point south) of cold dry air out of Canada (temperatures from −10–0°C, low dewpoints), which descends behind the cold front.

[14] Figure 2b shows the cyclone influence on meridional CO_2 transport at θ_e = 300K. Since poleward moving air originates at subtropical latitudes where air is warmer and moister than equatorward moving air, θ_e intersects the surface at higher latitude in the warm sector (~42°N) than the cold sector (~27°N). The primary pattern is for equatorward mass flux of low CO_2 air in the cold sector and poleward flux of high CO_2 air in the warm sector. As equatorward moving air sinks it crosses many pressure levels and creates large anomalous mass fluxes. Cold sector transport is dry; q is zero on θ_e and equatorward transport is equal on θ (not shown) and θ_e. Similarly, poleward moving air crosses many pressure levels during moist ascent, with equally large anomalous mass fluxes. Warm sector transport is moist and q is nonzero; since θ_e conserves energy in the presence of latent heating by condensation while θ gains energy, θ_e is more indicative of parcel trajectories along moist conveyors. This portion of eddy transport is parsed to the mean term when diagnosed on θ, reducing eddy CO_2 transport by nearly half (Figure 1d). Because covariance of CO_2 and mass flux is positive in the warm and cold sectors in the time and zonal mean at θ_e = 300K, net eddy transport over North America (N. A.) is poleward. Eddy transport over Eurasia, as well as along other θ_e surfaces, has different

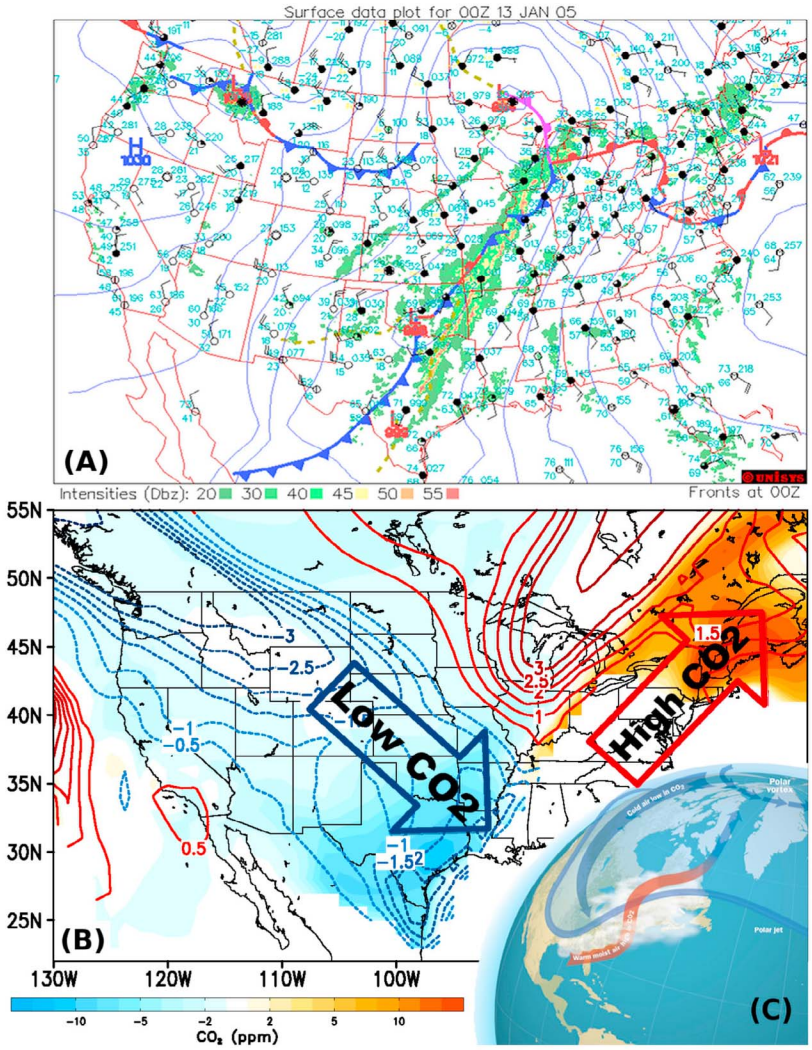

Figure 2. Case study from Jan 13, 2005 showing an example of eddy CO_2 transport associated with a typical midlatitude cyclone. (a) The surface composite map is reproduced with permission of Unisys Corporation © 2011. (b) Model output of anomalous CO_2 (C', ppm, shaded) and mass flux (mv', 1×10^{-4} kg m^{-1} s^{-1} K^{-1}, contour) along θ_e = 300K. (c) Inset illustrating key interactions between baroclinic wave and atmospheric CO_2 during boreal winter (courtesy Alex Reardon and Rod Paine).

latitudinal origins, with corresponding transport dependent on the latitudinal CO_2 gradient and the amount of convective instability of θ_e, but follows the same principle, leading to net column integrated zonal eddy transport according to Figure 1d. Eddy transport mechanisms are illustrated in Figure 2c.

[15] Stationary waves exhibit correlations between mass flux and CO_2 deviations ranging from 0.3–0.6 in northern middle latitudes while correlations within transient waves are closer to 0.15. Higher correlations in stationary waves suggest a strong and systematic correspondence between mass flux and CO_2 deviations, with net flow dominated by poleward transport of CO_2. Low correlations in transient waves suggest that transport by traveling cyclones is noisy and mixed between poleward and equatorward transport. Although net eddy transport is poleward in the time and zonal mean, instances of net equatorward transport inevitably arise (e.g., Figure 2b).

[16] Migrating cyclones responsible for CO_2 advection also cause a great deal of precipitation and cloudiness. In the case illustrated above, radar (color filled stippling in Figure 2a) indicates observed precipitation and filled surface stations cloudiness. Radar shows that precipitation during this day occurs primarily near cold and warm fronts. Surface station analysis indicates that moist conveyors in the warm sector are also very cloudy. Covariance among condensing air (i.e., clouds), precipitation, CO_2, and heat transport means that CO_2 transport along the east side of baroclinic waves will be hidden from satellite observing systems (see Figure 2c). Transport along the DI, however, is dry and sunny (open surface stations) and detectable by satellites.

[17] Meridional transport strongly mediates the seasonal cycle of CO_2 in mid-latitudes and amplifies it in high latitudes, accounting for most of the observed seasonality at sites like Barrow, Alaska and Alert, Canada [*Fung et al.*,

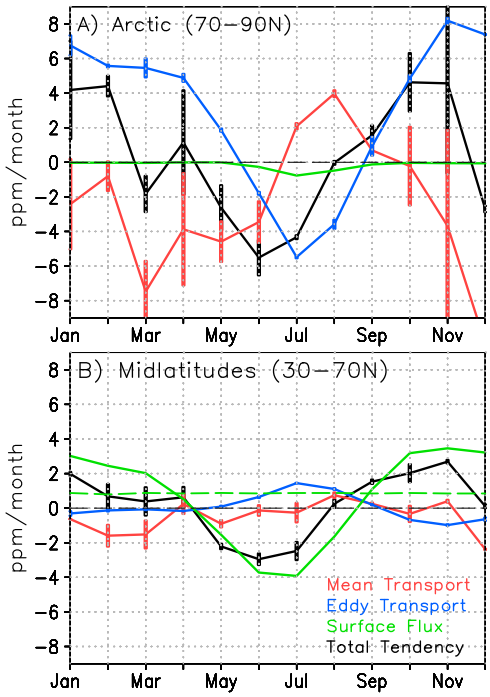

Figure 3. Column integrated seasonal CO_2 budget tendencies (ppm month^{-1}) on θ_e binned into (a) high latitudes and (b) mid-latitudes. Transport by transient and stationary eddies is plotted in blue, mean meridional transport in red, the total CO_2 tendency in black, and the total surface flux of carbon from land, ocean, and fossil fuels in green. The fossil fuel tendency is plotted as a dashed green line. The sum of individual tendencies (red, blue and green lines) is equal to the total tendency (black line). Error bars represent the root mean squared error.

1983]. Comparison of satellite observed vegetation with modeled transport implies that atmospheric mixing produces signals at high latitudes where vegetation is sparse [*Fung et al.*, 1987]. To convey the influence of eddy and mean transport on seasonality in the Arctic from a θ_e perspective, as well as extend findings of Figures 1 and 2 to all seasons, we plot the seasonal cycle of the atmospheric CO_2 tendency (tendencies in ppm month^{-1} are approximated by dividing equation (1) through by zonal and time averaged surface pressure) binned by latitude into the Arctic and mid-latitudes as a function of eddy transport, mean transport and surface flux tendencies (Figure 3).

[18] CO_2 seasonality is stronger in the Arctic despite weak surface fluxes (Figure 3a). This is driven strongly by synoptic eddies and therefore moist synoptic storms. Polar seasonality is strongly opposed by the mean meridional circulation, with net equatorward transport (at all northern latitudes) from September–June and poleward transport during summer. The same transport processes responsible for seasonality in the Arctic also strongly damp the seasonal cycle in mid-latitudes to about 50% of the seasonality implied by net ecosystem exchange, with eddy transport of similar magnitude to fossil fuel emissions during summer and fall (Figure 3b). Eddy transport tends to lead mean transport by 2–4 weeks during summer in the Arctic.

4. Discussion and Conclusions

[19] Synoptic eddies transport up to 1 PgC month^{-1} north and south in mid-latitudes. As a result, seasonality is strongly damped in mid-latitudes and amplified in polar latitudes. To put this in perspective, eddies transport more CO_2 out of mid-latitudes than is emitted by fossil fuels. Eddy transport is likely sensitive to model choice and should increase as models become more skilled at representing important eddy processes such as frontal circulation, moist convection and precipitation. Additionally, interannual variability in eddy (or mean) transport may contribute to trends in CO_2 seasonality in the Arctic [e.g., *Keeling et al.*, 1996], although such analysis is beyond the scope of this study. Because eddies mediate seasonality in northern latitudes, it is important for inversion scientists (modelers and observationalists) to consider them carefully.

[20] Sensitivity of eddy CO_2 transport to factors such as storm track position, seasonal tendencies in CO_2 mixing ratio and the pattern of seasonal change in surface CO_2 flux over the globe poses a challenging task for inversion modelers. Additionally, interpretation of synoptic variations in continental records requires accurate simulation of frontal weather systems [*Geels et al.*, 2004; *Wang et al.*, 2007; *Parazoo et al.*, 2008] and moist conveyors. As discussed in this study and by *Corbin and Denning* [2006], moist processes associated with synoptic weather systems hide much of the dynamics from satellites, and likely from other observing systems (e.g., aircraft flask samples [*Stephens et al.*, 2007]). Additionally, warm conveyors transport CO_2 and other trace gases into the polar vortex where they are hidden during polar winter. Continuous in-situ records can supplement airborne and remotely observed measurements during inclement weather, but only at a few locations. This fair-weather bias in measurements puts stringent requirements on models of moist transport. We therefore recommend that inversion modelers pay special attention to modeling of wet synoptic storms in addition to in-situ and satellite observations, with particular attention given to factors such as grid spacing (e.g., frontal circulations better resolved with finer grid spacing), representation of moist convection along fronts and within the warm sector of cyclones, and assimilation of observations of moisture.

[21] An additional complication arises in dry parts of the mid-latitude circulation where high-pressure systems transport CO_2 in different directions within an atmospheric column due to convergence aloft and divergence near the surface. Although column and in-situ measurements help constrain dry flow, there is over-reliance on models to distinguish between large and opposing directions of transport. Transport aloft, for example, is driven largely by deep tropical convection, which is typically parameterized in global transport models.

[22] It is important to correctly represent large-scale meridional CO_2 gradients flowing over regional domains because interaction with synoptic waves generates a source of variability that may confound flux attribution [*Keppel-Aleks et al.*, 2011]. The annual sink over N. A. varies by ~30% when lateral boundary conditions are prescribed from two different global transport models [*Schuh et al.*, 2010].

Because of large meridional transport by synoptic eddies, regional inversions should carefully account for meridional advection at north and south borders when prescribing lateral boundary conditions.

[23] Finally, it is worth exploring in more detail to what degree synoptic transport into the polar vortex influences equatorward moving air at a later point in time. Previous studies show that point emissions of tracer can scatter widely north, south, and across ocean basins through interaction with baroclinic waves [e.g., *Cooper et al.*, 2001, 2004]. It is common, for example, for baroclinic waves to advect polluted Asian air into the Arctic. A portion of this air is advected back south into N. A. with the same system, but the rest mixes in the polar vortex. Counter to intuition CO_2 anomalies in air arriving at mid-latitude sites from the north may actually reflect fluxes that occurred earlier to the south, and mixing with the polar vortex scrambles any coherent link between the longitudinal origin of poleward and equatorward moving air.

[24] **Acknowledgments.** This research is supported by the National Aeronautics and Space Administration contracts NNX08AT77G, NNX06AC75G, and NNX08AM56G.

[25] The Editor thanks two anonymous reviewers for their assistance in evaluating this paper.

References

Bethan, S., G. Vaughan, C. Gerbig, A. Volz-Thomas, H. Richer, and D. A. Tiddeman (1998), Chemical air mass differences near fronts, *J. Geophys. Res.*, *103*, 13,413–13,434, doi:10.1029/98JD00535.

Carlson, T. N. (1981), Speculations on the movement of polluted air to the Arctic, *Atmos. Environ.*, *15*, 1473–1477, doi:10.1016/0004-6981(81)90354-1.

Cooper, O. R., J. L. Moody, D. D. Parrish, M. Trainer, T. B. Ryerson, J. S. Holloway, G. Hubler, F. C. Fehsenfeld, S. J. Oltmans, and M. J. Evans (2001), Trace gas signatures of the airstreams within North Atlantic cyclones: Case studies from the North Atlantic Regional Experiment (NARE '97) aircraft intensive, *J. Geophys. Res.*, *106*, 5437–5456, doi:10.1029/2000JD900574.

Cooper, O. R., et al. (2004), A case study of transpacific warm conveyor belt transport: Influence of merging airstreams on trace gas import to North America, *J. Geophys. Res.*, *109*, D23S08, doi:10.1029/2003JD003624.

Corbin, K. D., and A. S. Denning (2006), Using continuous data to estimate clear-sky errors in inversions of satellite CO_2 measurements, *Geophys. Res. Lett.*, *33*, L12810, doi:10.1029/2006GL025910.

Denning, A. S., I. Y. Fung, and D. Randall (1995), Latitudinal gradient of atmospheric CO_2 due to seasonal exchange with land biota, *Nature*, *376*, 240–243, doi:10.1038/376240a0.

Doney, S. C., I. Lima, J. K. Moore, K. Lindsay, M. J. Behrenfeld, T. K. Westberry, N. Mahowald, D. M. Glover, and T. Takahashi (2009), Skill metrics for confronting global upper ocean ecosystem-biogeochemistry models against field and remote sensing data, *J. Mar. Syst.*, *76*, 95–112, doi:10.1016/j.jmarsys.2008.05.015.

Eckhardt, S., A. Stohl, H. Wernli, P. James, C. Forster, and N. Spichtinger (2004), A 15-year climatology of warm conveyor belts, *J. Clim.*, *17*, 218–237, doi:10.1175/1520-0442(2004)017<0218:AYCOWC>2.0.CO;2.

Fung, I., K. Prentice, E. Matthews, J. Lerner, and G. Russell (1983), Three-dimensional tracer model study of atmospheric CO_2: Response to seasonal exchanges with the terrestrial biosphere, *J. Geophys. Res.*, *88*, 1281–1294, doi:10.1029/JC088iC02p01281.

Fung, I. Y., C. J. Tucker, and K. C. Prentice (1987), Application of Advanced Very High Resolution Radiometer vegetation index to study atmosphere-biosphere exchange of CO_2, *J. Geophys. Res.*, *92*, 2999–3015, doi:10.1029/JD092iD03p02999.

Geels, C., S. C. Doney, R. Dargaville, J. Brandt, and J. H. Christensen (2004), Investigating the sources of synoptic variability in atmospheric CO_2 measurements over the Northern Hemisphere continents: A regional model study, *Tellus, Ser. B*, *56*, 35–50, doi:10.1111/j.1600-0889.2004.00084.x.

Kawa, S. R., D. J. Erickson III, S. Pawson, and Z. Zhu (2004), Global CO_2 transport simulations using meteorological data from the NASA data assimilation system, *J. Geophys. Res.*, *109*, D18312, doi:10.1029/2004JD004554.

Keeling, C. D., J. F. S. Chin, and T. P. Whorf (1996), Increased activity of northern vegetation inferred from atmospheric CO_2 measurements, *Nature*, *382*, 146–149, doi:10.1038/382146a0.

Keppel-Aleks, G., P. O. Wennberg, and T. Schneider (2011), Sources of variations in total column carbon dioxide, *Atmos. Chem. Phys.*, *11*, 3581–3593, doi:10.5194/acp-11-3581-2011.

Miyazaki, K., P. K. Patra, M. Takigawa, T. Iwasaki, and T. Nakazawa (2008), Global-scale transport of carbon dioxide in the troposphere, *J. Geophys. Res.*, *113*, D15301, doi:10.1029/2007JD009557.

Parazoo, N., A. S. Denning, R. Kawa, K. Corbin, R. Lokupitia, I. Baker, and D. Worthy (2008), Mechanisms for synoptic transport of CO_2 in the midlatitudes and tropics, *Atmos. Chem. Phys.*, *8*, 7239–7254, doi:10.5194/acp-8-7239-2008.

Pauluis, O., A. Czaja, and R. Korty (2008), The global atmospheric circulation on moist isentropes, *Science*, *321*, 1075–1078, doi:10.1126/science.1159649.

Peixoto, J. P., and A. H. Oort (1992), *Physics of Climate*, Am. Inst. of Phys., New York.

Schuh, A. E., A. S. Denning, K. D. Corbin, I. T. Baker, M. Uliasz, N. Parazoo, A. E. Andrews, and D. E. J. Worthy (2010), A regional high-resolution carbon flux inversion of North America for 2004, *Biogeosciences*, *7*, 1625–1644, doi:10.5194/bg-7-1625-2010.

Stephens, B. B., et al. (2007), Weak northern and strong tropical land carbon uptake from vertical profiles of atmospheric CO_2, *Science*, *316*, 1732–1735, doi:10.1126/science.1137004.

Stohl, A. (2001), A one-year Lagrangian "climatology" of airstreams in the Northern Hemisphere troposphere and lowermost stratosphere, *J. Geophys. Res.*, *106*, 7263–7279, doi:10.1029/2000JD900570.

Tans, P., I. Fung, and T. Takahashi (1990), Observational contrains on the global atmospheric CO_2 budget, *Science*, *247*, 1431–1438, doi:10.1126/science.247.4949.1431.

Townsend, R. D., and D. R. Johnson (1985), A diagnostic study of the isentropic zonally averaged mass circulation during the first GARP global experiment, *J. Atmos. Sci.*, *42*, 1565–1579, doi:10.1175/1520-0469(1985)042<1565:ADSOTI>2.0.CO;2.

Wang, J.-W., A. S. Denning, L. Lu, I. T. Baker, K. D. Corbin, and K. J. Davis (2007), Observations and simulations of synoptic, regional, and local variations in atmospheric CO_2, *J. Geophys. Res.*, *112*, D04108, doi:10.1029/2006JD007410.

J. A. Berry, Department of Global Ecology, Carnegie Institution of Washington, 260 Panama St., Stanford, CA 94305, USA.

A. S. Denning, N. C. Parazoo, and D. A. Randall, Department of Atmospheric Science, Colorado State University, 1371 Campus Delivery, Fort Collins, CO 80523-1371, USA. (nparazoo@atmos.colostate.edu)

S. C. Doney, Woods Hole Oceanographic Institution, 266 Woods Hole Rd., MS 25, Woods Hole, MA 02543, USA.

S. R. Kawa, NASA Goddard Space Flight Center, Code 613.3, Greenbelt, MD 20771, USA.

O. Pauluis, Courant Institute of Mathematical Sciences, New York University, New York, NY 10012, USA.

A. Wolf, Department of Ecology and Evolutionary Biology, Princeton University, Princeton, NJ 08544, USA.